Chemical Engineering Science, 1967, Vol. 22, pp. 1067–1078. Pergamon Press Ltd., Oxford. Printed in Great Britain.

The low temperature oxidation of ammonia over a supported ruthenium catalyst

T. J. SCHRIBER* and G. PARRAVANO

Department of Chemical and Metallurgical Engineering, University of Michigan
Ann Arbor, Michigan 48104

(*Received* 18 *November* 1966; *in revised form* 1 *February* 1967)

Abstract—The kinetics of the oxidation of NH_3 with O_2 over a 0·5 (wt.%) Ru catalyst supported on 0·318 (cm) cylindrical Al_2O_3 pellets has been studied in a stirred flow reactor with rapid recycling of 98 per cent or more of the reacting gas mixture. This experimental approach minimized temperature and concentration gradients along the cayalyst bed, and permitted fine temperature control and rapid mass transport to the catalyst surface. As a result, uniform reaction conditions prevailed over the length of the catalytic reactor.

Experimentation was conducted at six temperatures in the range 246–345 (°C). Reaction pressures from 176 to 280 (cm Hg) were used. Feed composition was 5·3, 9·7, or 16·5 (vol. %) NH_3, the balance in each case being O_2. The reactor effluent was analyzed by gas chromatography, and the products of reaction were N_2, N_2O and H_2O.

Rates of formation of both N_2 and N_2O were found to depend on p_{NH_3}, p_{O_2}, and p_{H_2O} and to be independent of p_{N_2} and p_{N_2O}. Increasing p_{H_2O} decreased, and increasing p_{O_2} increased, both rates. Increasing p_{NH_3} and temperature favored the formation of N_2O. The maximum N_2O yield realized in this work was about 45 per cent. Gas phase mass transport did not influence product distribution and did not control the reaction rate.

Equations are developed to express the rates of formation of N_2 and N_2O. These rate equations are discussed in terms of a kinetic scheme involving two parallel reactions with O_2 as a common reagent. Possible elementary steps, which constitute both oxidation reactions, are analyzed in relation to the experimentally derived rate expressions. The latter are compared with those predicted by absolute rate theory and order-of-magnitude agreement results.

A LARGE body of information is presently available on the catalytic, high temperature [>400 (°C)] oxidation of NH_3 to N_2, NO, NH_2OH and H_2O [1]. The low temperature raction, whose significant products are N_2, N_2O and H_2O, has not received a comparable amount of attention and no kinetic analysis of it has been carried out [2]. In principle the relationship among N_2, N_2O and NH_3 can be represented by:

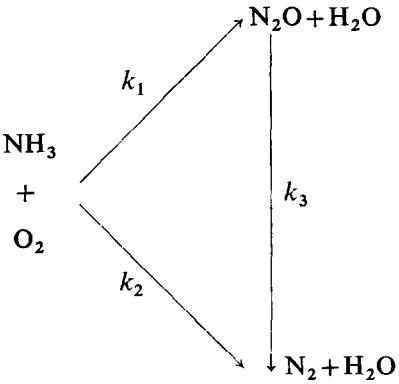

(1)

* National Science Foundation Predoctoral Fellow 1958–1961; present address: Eastern Michigan University, Ypsilanti, Michigan.

In catalytic reactions, this scheme must include adsorption, desorption and surface reaction steps of all reactants and products, giving rise to a variety of reaction mechanisms and controlling steps [3]. To gather information on this problem and analyze the validity of various kinetic schemes, we have performed experiments on the rate of the catalytic oxidation of NH_3 on a supported Ru catalyst. The study was performed in the temperature range 246–345 (°C), p_{NH_3} 1·1–44·1 (mm Hg), p_{O_2} 67·2–269·8 (mm Hg), total pressure up to 4 (atm). Under these conditions, it was found that $k_3 \ll k_2$; thus the oxidation can be simply represented by two parallel reactions occurring on the Ru surface without competition between O_2 and NH_3. Equations describing the experimental rates of formation of N_2 and N_2O have been developed, and compared with expressions derived from different kinetic models.

EXPERIMENTAL

Materials

Ruthenium was chosen as a catalyst because of the relatively small amount of information available on its performance as an inorganic oxidation agent. Ru is known as a mild catalyst for organic oxidations [4], the water gas shift reaction [5], and the decomposition of NH_3 [6]. In addition, O_2 chemisorption readily occurs on RuO_2 [7], which is probably present on the metal surface in contact with an O_2 rich atmosphere.

The catalyst used in this study was obtained from a commercial source and consisted of 0·5 (wt.%) Ru on $\frac{1}{8}$in. pellets of γ-Al_2O_3. Physical properties of the catalyst are summarized in Appendix A. All gases used were from commercially available sources.

Because of the need to obtain a rather accurate account of product distribution as a function of the degree of conversion, a recirculation type of reactor was used and experimental conditions set up in such a manner that the maximum amount of NH_3 reacted across the catalyst bed of 5·1 (cm) in depth never exceeded 2 per cent. Further advantages of this type of reactor were good temperature control for the highly exothermic oxidation [303 (kcal mole^{-1})] (Appendix B), high mass transfer rates with low fresh feed rates (Appendix B), and direct measurement of reaction rate, eliminating the need to integrate the proposed rate equations. The experimental setup is schematically shown in Fig. 1. It included flow meters, molten salt bath for reactor heating, back pressure regulator, recycle pump, surge cylinders and sample valve. The reactor itself consisted of three 7·5 (cm) lengths of stainless steel tubing, 0·935 (cm) o.d. × 0·525 (cm) i.d., connected in series by two loops of 0·625 (cm) o.d. stainless steel tubing. Each length of tubing was fitted at the bottom with a perforated stainless steel disk which served to support the catalyst. To measure the temperature at each disk, thermocouple probes were inserted in each tube. To check the effect of mass transfer a second reactor of smaller diameter was used. In this manner the mass-transfer coefficient could be changed without varying the recycle rate. Since the recycling gases removed about 90 per cent of the heat of reaction from the catalyst section, changing the recycle rate at a fixed feed rate could have resulted in a variation of reaction temperature sufficient to mask mass-transfer effects. The recycle pump was a diaphragm compressor capable of up to 360 strokes/min.

The analysis of the products was performed by gas chromatography. One sample was used for the separation and analysis of O_2 and N_2 while in a second sample N_2O was separated from the effluent stream and the amount determined. With the aid of stoichiometric considerations the complete composition of the reactor effluent could be calculated. The assumption that the composition of both samples, taken a short interval of time apart, was the same is justified since all data were taken only after a steady reaction state was reached. A potentiometric recorder and integrator were used for the final computation of compositions. Additional details on the experimental setup can be found elsewhere [8].

Procedure

The feed mixture was prepared by premixing O_2 and NH_3 in appropriate cylinders. The composition of these mixtures was periodically checked by mass spectrometric and Burrel gas analysis. Helium was used as a diluent. No oxides of nitrogen were detected in the reactor effluent up to temperatures of 400 (°C)and feed rates of 200 (cm^{3}min^{-1}) with

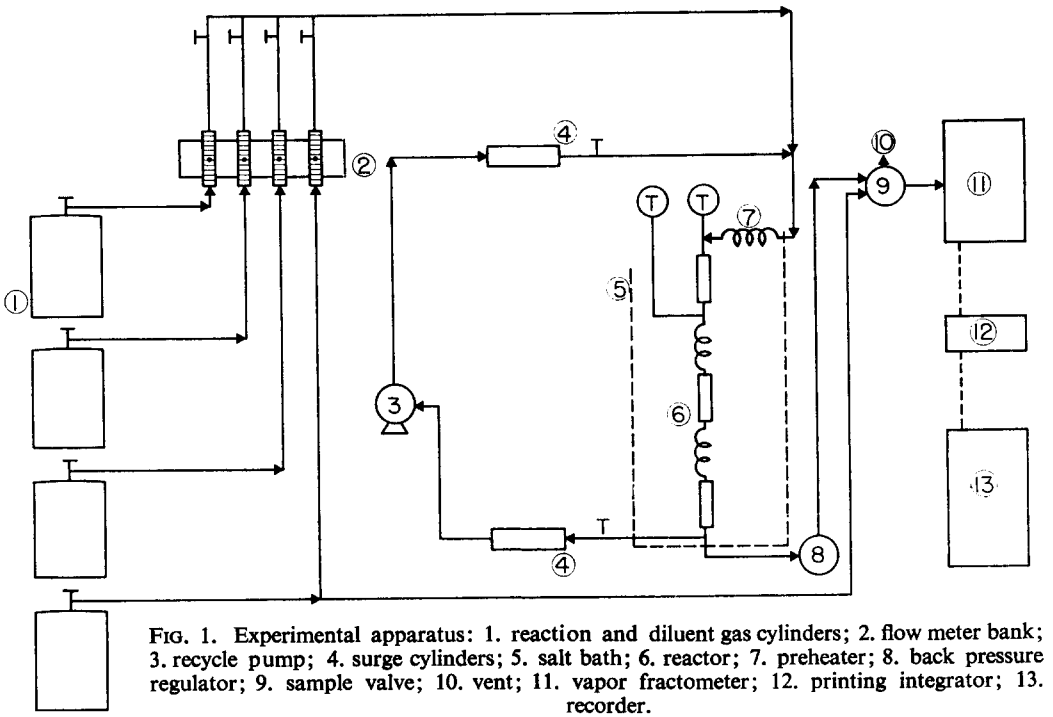

FIG. 1. Experimental apparatus: 1. reaction and diluent gas cylinders; 2. flow meter bank; 3. recycle pump; 4. surge cylinders; 5. salt bath; 6. reactor; 7. preheater; 8. back pressure regulator; 9. sample valve; 10. vent; 11. vapor fractometer; 12. printing integrator; 13. recorder.

the reactor empty or filled with Al_2O_3 pellets, identical to those used for catalyst support. It was further established that up to the same temperature no decomposition of H_2O upon the Al_2O_3 pellets occurred. No catalyst pretreatment was performed. Reaction rates at different feed rates were measured for each feed composition, reaction temperature and pressure. The order of runs followed was one of increasing contact time. After completing a series of runs, the system was evacuated and another series using a different feed composition was started. In all cases, the product consisted of N_2, N_2O and H_2O. The temperature range investigated was 243–345 (°C), the total pressure range 1–4 (atm), the volumetric flow rate $(2–9)\times10^2$ (cm^3STP min^{-1}) and the ratio of recycle rate/feed rate $(0{\cdot}5–3)\times10^2$.

The results of tests conducted to determine the constancy of the catalytic activity are presented in Fig. 2. These tests were also used to verify the validity of stirred flow conditions of the reactor. The results in Fig. 2 show that, under the experimental conditions used, no measurable compositional difference between upstream and downstream flows

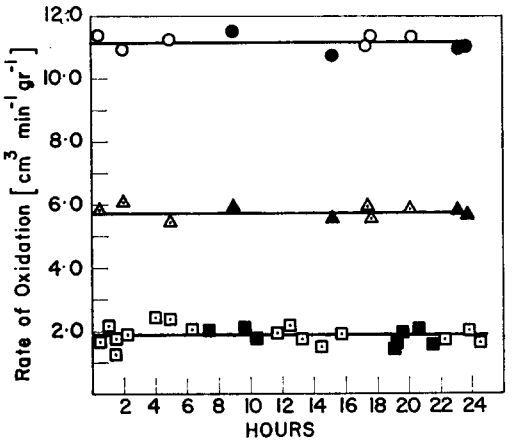

FIG. 2. Stability of catalytic activity: □ N_2 formation, 246 (°C), 357 (cm^3 min^{-1}), 9·7% NH_3; ○ N_2 formation, 322 (°C), 925 (cm^3 min^{-1}), 16·5 (vol.%) NH_3; △ N_2O formation, 322 (°C), 923 (cm^3min^{-1}), 16·5 (vol. %) NH_3; light mark, reactor downstream; solid mark, reactor upstream.

existed. Several runs were also performed to determine the reproducibility of measurements with different catalyst charges. In general the percentage deviation in the rate of N_2 production among several runs, performed under similar experimental

conditions, was about 2–3 per cent, while the same deviation for H_2O was 5 per cent. In order to test the influence of the reaction and product gases on the rate of oxidation, it was necessary to perform runs at different partial pressures of the component tested. For H_2O, this condition was established in two ways: (a) by setting $p_{H_2O} \approx 0$ by adsorption of the H_2O produced on Al_2O_3 pellets, inserted in the surge cylinder downstream from the reactor (the condition of $p_{H_2O} \approx 0$ was checked analytically), and (b) by directly establishing reaction conditions for which the partial pressures of O_2 and NH_3 were held approximately constant while the partial pressure of H_2O was varied. This was accomplished by using different feed compositions and permitting the reaction to proceed to various degrees of completion as a function of feed composition. Proper adjustment of total reaction pressure then made it possible to make measurements for which the partial pressure of H_2O varied while the partial pressures of O_2 and NH_3 were at fixed values. Results from these measurements were in excellent agreement with results in which the effect of H_2O was not studied directly. Water was found to inhibit the rates of formation of both H_2 and N_2O. The quantitative extent of inhibition was found to be exactly the same for both of the parallel reactions. In order to prevent H_2O condensation, the recycle loop and analysis outlet were continuously kept above room temperature.

EXPERIMENTAL RESULTS

Some typical results on the effect of contact time and temperature are presented in Fig. 3. The influence of p_{NH_3} on the overall rate of oxidation is shown in Figs. 4 and 5. The results show that the rate increased with increasing p_{NH_3}. The effect of p_{NH_3} upon the rate of formation of N_2 and N_2O at constant p_{O_2} and p_{H_2O} is shown in Figs. 6 and 7. The results of runs carried out to test the effect of p_{O_2} on the rates of N_2 and N_2O formation are presented in Figs. 8 and 9. The effect of p_{N_2} and p_{N_2O} on the rate of oxidation was investigated by adding N_2 and N_2O directly to the feed and raising, accordingly, the reaction pressure at temperatures of 295, 311 and 345 (°C). Typical results of these runs are presented in Fig. 10. The results of runs performed to test the influence of H_2O are reported in Figs. 11 and 12. In all cases, increasing p_{H_2O} decreased to the same extent the rates of formation of N_2O and N_2. An inspection of Figs. 9 and 10 shows that a similar conclusion applies to the influence of O_2 on both oxidation rates.

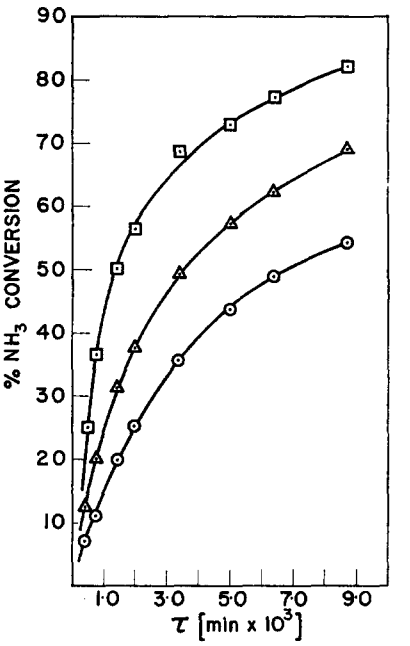

FIG. 3. Influence of contact time, τ, and temperature on NH_3 oxidation: P=3 (atm), 9·7 (vol. %) NH_3: ○ 273; △ 296; □ 322 (°C).

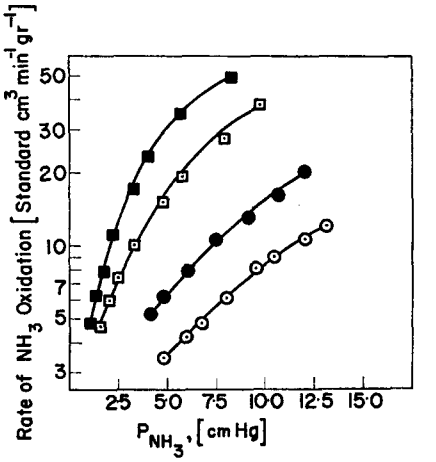

FIG. 4. Influence of p_{NH_3}, on the total rate of NH_3 oxidation, 280 (cm Hg), 5·3 (vol. %) NH_3 in feed; ○ 273; ● 296; □ 322; ■ 345 (°C).

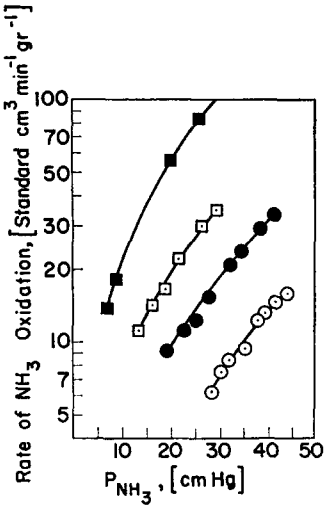

FIG. 5. Influence of p_{NH_3} on the total rate of NH_3 oxidation, 280 (cm Hg), 16·5 (vol. %) NH_3 in feed; ○ 246; ● 275; □ 296; ■ 322 (°C).

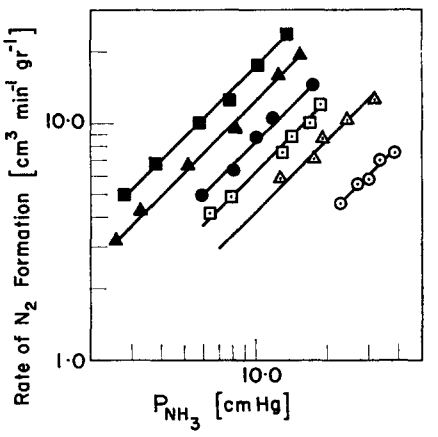

FIG. 6. Influence of p_{NH_3} on the rate of N_2 formation (H_2O removed from recycle); ○ 246; △ 273; □ 296; ● 311; ▲ 322; ■ 345 (°C).

The experimental results just described can be satisfactorily represented by the following empirical rate expressions:

$$r_{N_2} = (k_0)_{N_2} p_{NH_3} p_{O_2}^{0.46} p_{H_2O}^{-0.40} \quad (2)$$

$$r_{N_2O} = (k_0)_{N_2O} p_{NH_3}^{1.35} p_{O_2}^{0.46} p_{H_2O}^{-0.40} \quad (3)$$

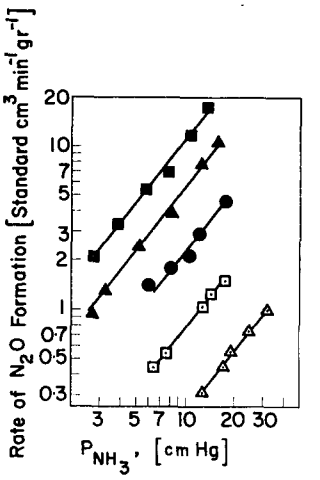

FIG. 7. Influence of p_{NH_3} on the rate of N_2O formation (H_2O removed from recycle); △ 273; □ 296; ● 311; ▲ 322; ■ 345 (°C).

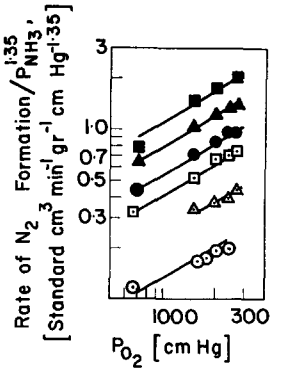

FIG. 8. Influence of p_{O_2} on the rate of N_2 formation (H_2O removed from recycle); ○ 246; △ 273; □ 296; ● 311; ▲ 322; ■ 345 (°C).

The influence of mass transfer on the rate of reaction was checked by varying the mass-transfer coefficient through variations of the cross section area of the reactor under otherwise identical reaction conditions. The effect was investigated at 345 (°C) since if mass transfer were without influence on the rate of reaction at this temperature, it would also be without influence at lower reaction rates corresponding to lower temperatures. By substituting a 0·390 (cm) diameter reactor for the 0·525 (cm) diameter reactor, the mass-transfer coefficient was

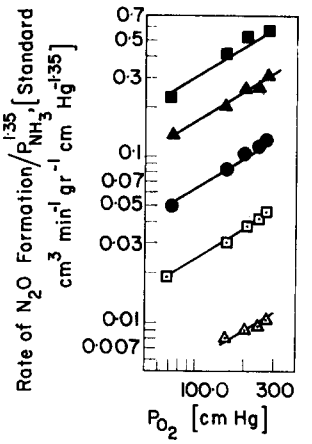

FIG. 9. Influence of p_{O_2} on the rate of N_2O formation (H_2O removed from recycle); △ 273; □ 296; ● 311; ▲ 322; ■ 345 (°C).

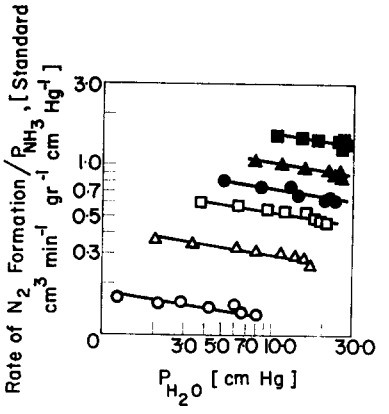

FIG. 11. Influence of p_{H_2O} on the rate of N_2 formation; ○ 246; △ 273; □ 296; ● 311; ▲ 322; ■ 345 (°C).

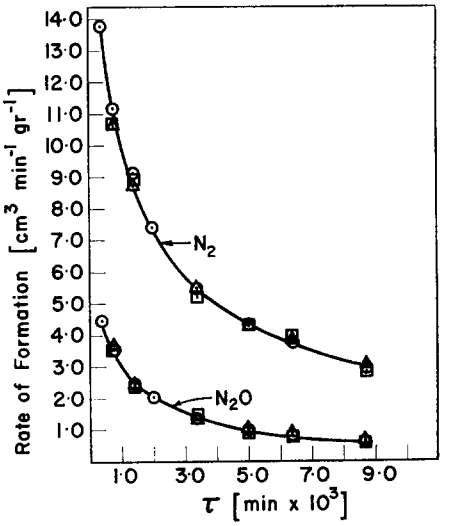

FIG. 10. Influence of p_{N_2} and p_{N_2O} on the rate of product formation at 311 (°C), $p=3$ (atm); ○ no N_2 or N_2O added to feed; △ N_2 added to feed; □ N_2O added to feed.

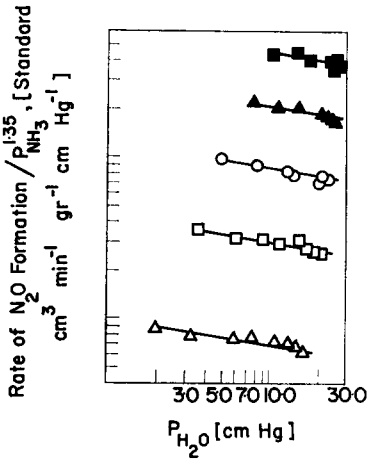

FIG. 12. Influence of p_{H_2O} on the rate of N_2O formation; △ 273; □ 296; ○ 311; ▲ 322; ■ 345 (°C).

increased by 35 per cent. Figure 13 shows that the measurements were not dependent upon the rate of mass transfer.

The variations associated with the exponents of Eqs. (2) and (3) where determined by means of the following mathematical procedure: using all possible combinations of four experimental measurements at each temperature, the values of the three exponents and k_0 were computed and the average values of each of these constants determined. The degree of variation of the average values was taken as that corresponding to the 95 per cent confidence limit of the numerical values computed in the initial step. These limits fall within plus or minus one degree of variation of the average values computed in the second step. The results of these computation were as follows: NH_3: $1{\cdot}00\pm0{\cdot}05$ (N_2 formation), $1{\cdot}35\pm0{\cdot}07$ (N_2O formation); O_2:$0{\cdot}46\pm0{\cdot}06$; H_2O:$-0{\cdot}40\pm0{\cdot}04$.

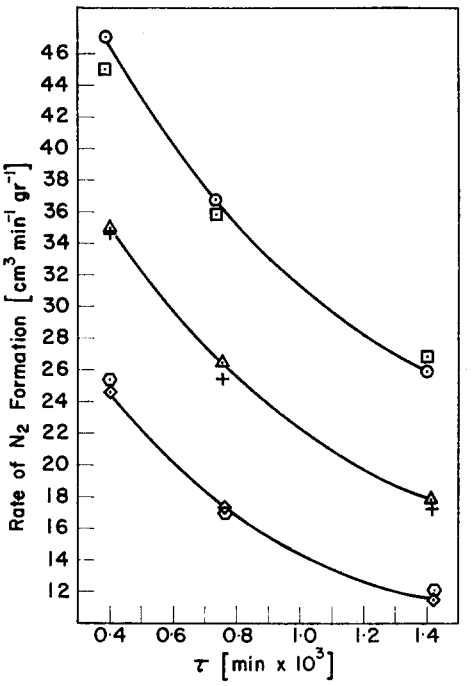

FIG. 13. Influence of Reynolds number on the rate of oxidation of NH_3, 345 (°C), 2·4 (atm), 16·5 (vol.%) NH_3; Reynolds number ⊙ 5·920, □ 19,200; 3 (atm), 9·7 (vol. %) NH_3; Reynolds number △ 6820 +22,100; 4 (atm), 5·3 (vol. %) NH_3; Reynolds number ◆ 7900, ● 25,600.

DISCUSSION

Since the experimental results have shown that $k_3 \approx 0$ [reaction scheme (1)], it is clear that the overall oxidation should be described by two parallel reactions yielding N_2O and N_2, respectively. Each reaction results from a sequence of elementary steps involving adsorption, surface reaction and desorption. With the help of the reported experimental results, it is possible to obtain some insight on the nature of the elementary steps.

In carrying out this task we shall initially consider the case that the establishment of surface reaction equilibria occurs without any complicating factor resulting from surface effects. Let us assume that the first steps involve the formation of nitroxyl, HNO, and imide, NH, surface radicals:

$$NH_3(g) \underset{k_5}{\overset{k_4}{\rightleftharpoons}} NHO(a)+H_2O(g) \quad (4)$$

$$+$$

$$O_2(g) \underset{k_5}{\overset{k_4}{\rightleftharpoons}} NH(a)+H_2O(g) \quad (5)$$

It is further assumed that NHO and NH are the only adsorbed species of interest, and that their surface concentrations, θ_{NHO}, θ_{NH} are controlled by equilibria (4) and (5) and that $\theta_{NH}=\alpha\theta_{NHO}$, where $\alpha=f(T)$. The fraction of free surface is then $\theta_f = 1-\theta_{NHO}-\theta_{NH}$.

Under these conditions, the rate of formation of N_2O follows from step (4) by means of:

$$NH_3(g)+NHO(a)\rightarrow N_2O(g)+4H(a) \quad (6)$$

where H(a) is desorbed as H_2O. The rate of reaction (6) is given by:

$$r_{N_2O}=k_{N_2O}p_{NH_3}\theta_{NHO}=k_{N_2O}p_{NH_3}\frac{1}{1+\alpha}$$

$$\times\left[\frac{(1+\alpha)K_4^* p_{NH_3}\dfrac{p_{O_2}}{p_{H_2O}}}{1+(1+\alpha)K_4^* p_{NH_3}\dfrac{p_{O_2}}{p_{H_2O}}}\right]$$

$$\cong k_{N_2O}(1+\alpha)^{-\frac{1}{2}}K_4^{*\frac{1}{2}}p_{NH_3}{}^{1\cdot5}p_{O_2}{}^{\frac{1}{2}}p_{H_2O}{}^{-\frac{1}{2}} \quad (7)$$

where $K_4^*=K_4^{-1}$.

Similarly, the rate of formation of N_2 follows reaction (5) by means of:

$$2NH\rightarrow N_2+H_2 \quad (8)$$

The rate of reaction (8) is given by:

$$r_{N_2}\cong k_{N_2}\theta_{NH}^2$$

$$=k_{N_2}\left(1+\frac{1}{\alpha}\right)^{-1}K_5^* p_{NH_3}p_{O_2}{}^{\frac{1}{2}}p_{H_2O}{}^{-1} \quad (9)$$

By comparing expressions (7) and (9) with the experimental rate equations (2) and (3) it is apparent that differences in the values of the exponents exist, the most serious one being that related to the effect of H_2O on r_{N_2}. Confronted with this situation, one may be tempted to assume other equilibrium and rate controlling steps, while still neglecting the possibility that surface effects may influence the establishment of surface equilibria. Thus, instead of Eq. (5), one can visualize the surface dissociation of NH_3 yielding NH_2 (with or without the direct participation of O_2), followed by a surface rearrangement of the adsorbed NH_2 fragment to yield N_2. However, the discrepancy between the calculated exponent for p_{H_2O} in the resulting rate expression and the experimental value will still be present. For other schemes the discrepancy in the O_2 exponent will become larger. Thus, it is not too helpful to try to improve the consistency of the assumed reaction scheme in this direction. On the other end, since the experimental technique used in this study allowed the establishment of a reaction conversion level within narrow limits for long periods of time, the values of the exponents in the rate Eqs. (2) and (3) can be trusted with a high degree of accuracy. Thus, the differences between experimental and calculated values are larger than any conceivable experimental error. Clearly, this situation indicates that the neglect of surface effects in the formulation of equilibria (4) and (5) is not an entirely valid procedure. In order to take this fact into account a choice among several possibilities should be made. However, the nature of the experimental results is such that the latter do not permit sufficient resolution and discrimination. The assumption of a catalyst surface, composed of two separate and independent sets of sites for the adsorption of NH_3 and for that of O_2 and H_2O may be made. Taking a simple Langmuir behavior for all three adsorptions, it is of course possible to calculate constants which would give an accurate fit of the experimental results. A qualitative justification for this procedure can be obtained by computing, from the temperature dependence of the adsorption constants, the heats and entropies of adsorption. This has been carried out [8] and the values obtained were found consistent with the expected theoretical quantities. In particular, the calculation of the adsorption entropies showed that the assumption of localized adsorption is valid for O_2, while it is doubtful for H_2O, unless the additional assumption is made that the adsorbed molecules gain vibrational degrees of freedom.

The empirical rate Eqs. (2) and (3) may be compared with expressions derived by absolute rate theory [9]. The latter gives for the present case:

$$(k_0)_{N_2\,\text{theo}} = \frac{kT}{h}\exp\left\{\frac{aF_{NH_3} + bF_{O_2} + cF_{H_2O}}{R}\right\} \quad (10)$$

$$(k_0)_{N_2O\,\text{theo}} = \frac{kT}{h}\exp\left\{\frac{dF_{NH_3} + eF_{O_2} + fF_{H_2O}}{R}\right\} \quad (11)$$

where the values of the constants a, b, c, d, e and f are those used in the empirical power rate expressions (2) and (3) for the corresponding chemical species.

By means of known values of the free energy functions F, [8], $(k_0)_{N_2\,\text{theo}}$, $(k_0)_{N_2O\,\text{theo}}$ have been

TABLE 1. VALUES† OF $k^0 = \dfrac{r \exp\{E/RT\}}{p_{NH_3}^{\,a} p_{O_2}^{\,b} p_{H_2O}^{\,c}}$ (molecules, site $^{-1}$, sec^{-1}), T=296 (°C)

	Experimental	Theoretical
Formation of N_2	$7{\cdot}85 \times 10_2$ [Eq. (12)]	$3{\cdot}6 \times 10^2$ [Eq. (10)]
Formation of N_2O	$4{\cdot}3 \times 10^9$ [Eq. (13)]	$5{\cdot}4 \times 10^8$ [Eq. (11)]

† In this calculation it was assumed that the number of reaction sites was given by the number of Ru atoms. The latter when dispersed on a monolayer would occupy an area given by:

$$S = \frac{N^{\frac{1}{3}} w}{\rho^{\frac{1}{3}} M^{\frac{1}{3}} 10^4 W} = 5 \times 10^{-3}\,(6{\cdot}023 \times 10^{23})^{\frac{1}{3}} = 1{\cdot}71\ (\text{m}^2\text{g}^{-1}).$$

The area of the $\gamma - Al_2O_3$ support was about 120 (m^2 g^{-1}).

evaluated (Table 1). The corresponding experimental quantities were computed by means of the expressions:

$$(k_0)_{N_2\,exp}=\frac{r_{N_2O}\exp\left\{\frac{E_{N_2}}{RT}\right\}}{p_{NH_3}p_{O_2}^{0.46}p_{H_2O}^{-0.40}} \quad (12)$$

$$(k_0)_{N_2O\,exp}=\frac{r_{N_2O}\exp\left\{\frac{E_{N_2O}}{RT}\right\}}{p_{NH_3}^{1.35}p_{O_2}^{0.46}p_{H_2O}^{-0.40}} \quad (13)$$

Using the experimentally determined values, $E_{N_2}=12{\cdot}6$ (kcal mole^{-1}), $E_{N_2O}=35{\cdot}0$ (kcal mole^{-1}), $(k_0)_{N_2exp}$ and $(k_0)_{N_2O\,exp}$ were computed at 296°C from Eqs. (12) and (13) (Table 1). The theoretical and experimental values of k_0 are within one order of magnitude. Hence, the measured rates are in satisfactory agreement with rates predicted through the application of absolute rate theory.

Conclusions

The catalytic, low temperature oxidation of NH_3 over a Ru catalyst, supported on $\gamma-Al_2O_3$, may be described by two parallel, competitive reactions yielding N_2O and N_2, respectively. The slow reaction steps involve the dimerization of surface imide groups and the reaction between NH_3 and adsorbed nitroxyl groups. The rate of N_2 production is first order to p_{NH_3} while that of N_2O formation is dependent upon $p_{NH3}^{1.35}$. Taking into consideration the presence of surface effects in the adsorptions of O_2 and H_2O, it is possible to calculate ΔS of adsorption for both species. The calculation shows that adsorbed O_2 is relatively immobile and localized, while it is doubtful whether the same conclusion can be applied to adsorbed H_2O.

Acknowledgment—This research was supported by financial grants from the International Nickel Company and the Air Force Office of Scientific Research. The authors acknowledge this support with thanks.

Notation

- a NH_3 exponent in power rate expression, N_2 results
- a_m external catalyst pellet area per unit mass
- a_p external catlyst pellet area per pellet
- b O_2 exponent in power rate expression, N_2 results
- C_p heat capacity
- c H_2O exponent in power rate expression, N_2 results
- D reactor diameter
- D_A diffusivity of component A
- d NH_3 exponent in power rate expression, N_2O results
- E activation energy
- e O_2 exponent in power rate expression, N_2O results
- f H_2O exponent in power rate expression, N_2O results
- F free energy function
- G superficial mass velocity
- h Planck's constant
- j_D j-factor for mass transfer
- K reaction equilibrium constant
- $(k_0)_A$ overall rate coefficient in rate equation for formation of species A
- k thermal conductivity
- k Boltzmann's constant
- M_m average molecular weight of gas
- N Avogadro number
- p total gas pressure
- p_A partial pressure of gas species A
- p_f gas film pressure
- R gas constant
- r rate of reaction
- ΔS area occupied by Ru atoms
- S adsorption entropy
- T temperature
- w weight of Ru in catalyst (%)
- W weight of catalyst support
- α constant
- μ viscosity
- θ_A fraction of catalyst surface covered with A
- ρ density
- τ contact time

References

[1] Andrussow L., *Angew. Chem.* 1926 **39** 321; 1927 **40** 174; 1928 **41** 207; *Chemie-Ingr-Tech.* 1955 **27** 469.
Bodenstein M., *Angew. Chem.* 1927 **40** 174; *Z. Elektrochem.* 1935 **41** 466.
Bodenstein M. and Buettner G., *Angew. Chem* 1934 **47** 364.
Krauss W., *Z. Elektrochem.* 1950 **54** 264.
Krauss W. and Schuleit H., *Z. Phys. Chem.* 1939 **B45** 1.
Kuhlman K., *Justus Liebigs Annln Chem.* 1939 **29** 281.
Raschig F., *Angew. Chem.* 1928 **41** 1183; *Z. phys. Chem.* 1938 **B41** 75.
Zawadzki J., *Trans. Faraday Soc., Disc.* 1950 **No. 8** 140.

[2] VON NAGEL A., *Z. Elecktrochem.* 1930 **36** 754.
KRAUSS W. and NEUHAUS A., *Z. Phys. Chem.* 1941 **B50** 323.
GIORDANO N., CAVATERRA E. and ZEMA D., *Chimica Ind., Milano* 1963 **45** 14.
[3] DEBOER J. H. and VAN DER BORG, R.J.A.M. in *Actes du Deuxième Congrès International de Catalyse*, p. 919. Technip, Paris, 1960.
[4] PARRAVANO G. and MORENO V., *Gazz. Chim. Ital.* 1961 **91** 479.
[5] PARRAVANO G., *Ind. Engng Chem.* 1957 **49** 266.
[6] AMANO A. and TAYLOR H. S., *J. Am. Chem. Soc.* 1954 **76** 4201.
[7] SOMMERFELD J. T. and PARRAVANO G., *J. Phys. Chem.* 1965 **69** 102.
[8] SCHRIBER T. J. Ph.D. Thesis, University of Michigan 1964.
[9] VAN REIJEN L. L. and SCHULT G., *Bull. Soc. Chim. Belge* 1958 **67** 489.
[10] YANG K. H. and HOUGEN O. A., *Chem. Engng Prog.* 1950 **46** 146.

APPENDIX A

Physical properties of the ruthenium catalyst

Pellet diameter (cm)	0·318
Pellet length (cm)	0·318
Bulk density (g cm^{-3})	0·93
Particle density (g cm^{-3})	1·67
True density (g cm^{-3})	3·40
Internal void fraction	0·56
External void fraction	0·54

APPENDIX B

Calculation of pressure and temperature drop between bulk gas and catalyst surface

The following expressions are used to compute the expected pressure drop,

$$\frac{\Delta p_A}{p_A}$$

due to diffusion from the bulk of the phase to the exterior catalyst surface [10]:

$$\frac{\Delta p_A}{p_A}=\left(\frac{r}{p_A}\right)=\left(\frac{p_f(a_p)^{\frac{1}{2}}M_m}{1{\cdot}24\mu a_m}\right)\left(\frac{\mu}{\rho D_{Am}}\right)^{\frac{2}{3}}\left(\frac{(a_p)^{\frac{1}{2}}G}{\mu}\right)^{-0{\cdot}59} \quad (14)$$

At 345·5 (°C) the maximum ratio of reaction rate to p_{NH_3} occurred. At this temperature, using the values listed in Table 2 and using

$$\frac{r}{p_A}=5{\cdot}88[\mathrm{cm^2\,min^{-1}\,g^{-1}\,cm^{-1}}]$$

(the largest used) it is found

$$\frac{\Delta p_A}{p_A}=0{\cdot}0133.$$

Thus, the pressure drop is 1·5 per cent of the bulk p_{NH_3} for the most rapid rate of NH_3 oxidation encountered in this study. Assuming that Ru metal is evenly distributed on the Al_2O_3 pellet, the deposition of 0·5 (wt. %) Ru corresponds to a penetration of 0·2 per cent into pellet interior, indicating that pore diffusion can hardly be considered a limiting factor.

The temperature difference ΔT, between the main gas stream and the catalyst surface was calculated by means of the equation [10]:

$$\frac{\Delta T}{T}=\left(\frac{r}{T}\right)\left(\frac{\Delta H(a_p)^{\frac{1}{2}}}{1{\cdot}35\mu c_p a_m}\right)\left(\frac{c_p\mu}{k}\right)^{\frac{2}{3}}\left(\frac{(a_p)^{\frac{1}{2}}G}{\mu}\right)^{-0{\cdot}59} \quad (15)$$

This equation has been evaluated at 345 (°C) where the maximum rate and thus the maximum ΔT was encountered. The numerical values used are listed in Table 2. The maximum rate of oxidation was found at a reaction pressure of 176 (cm Hg). In this instance, Eq. (15) yields

$$\frac{\Delta T}{T}=0{\cdot}0175,$$

or a temperature differential of about 1·1°C existed between the catalyst surface and the bulk gas stream. Despite the crudeness of this calculation, it indicates that no large temperature gradients were present. This conclusion was to some extent confirmed experimentally by measuring the catalyst temperature at 345·5 (°C), in a small hole, bored in the bottom of a pellet contacted by the reactant stream. A thermocouple positioned in this hole showed a temperature 0·6 (°C) less than the exit gas stream temperature.

TABLE 2. NUMERICAL VALUES USED IN EQS. (14) AND (15)

Value	Comment
$\mu = 0{\cdot}034$ (g cm^{-1} sec^{-1})	Viscosity of O_2 used to approximate gas mixture viscosity
$M_m = 29$	Average molecular weight of the gas
$\rho = 8{\cdot}23\ p \times 10^{-6}$ [g cm^3 cm Hg^{-1}]	Density as a function of reaction pressure p, (cm Hg)
$D_{NH_3} = 0{\cdot}0126p$(cm^2 sec^{-1} cm Hg^{-1})	Diffusivity of NH_3 in O_2 approximated to diffusivity of NH_3 in air, as a function of reaction pressure p (cm Hg)
p_f, p (atm)	Gas film pressure taken equal to reaction pressure
$a_p^{\frac{1}{2}} = 0{\cdot}685$ (cm)	Pellet area taken equal to the surface area of a $0{\cdot}318 \times 0{\cdot}318$ (cm^2) cylinder
$a_m = 11{\cdot}0$ (cm^2 g^{-1})	External surface area per pound of pellets
$G = 4{\cdot}8$ (g sec^{-1} cm^{-2})	Mass rate at reaction pressure 2·32 (atm)
$G = 5{\cdot}55$ (g sec^{-1} cm^{-2})	Mass rate at reaction pressure 2·84 (atm)
$G = 6{\cdot}45$ (g sec^{-1} cm^{-2})	Mass rate at reaction pressure 3·68 (atm)
$C_p = 0{\cdot}45$ (cal g^{-1} °C^{-1})	Heat capacity (O_2)
$k = 1{\cdot}97 \times 10^{-4}$ (cal sec^{-1} cm^{-1} °K^{-1})	Thermal conductivity (O_2)
$\frac{C_p\mu}{k} = 0{\cdot}77$	Prandtl number taken equal to that for air

Résumé—La théorie cinétique de l'oxydation de NH_3 par O_2 sur un catalyseur 0,5 (% par poids) Ru contenu dans des pastilles de Al_2O_3 cylindriques de 0,318 cm, a été étudiée dans un réacteur à courant agité avec un recyclage rapide à 98% du mélange gazeux de réaction. Ce procédé expérimental a réduit les pentes de température et de concentration le long du lit du catalyseur, et permis un bon contrôle de la température et un transport rapide de la masse à la surface du catalyseur. En résultat, les conditions uniformes de réaction l'ont emporté sur la longueur du réacteur de catalyse.

L'expérience a été faite à six températures dans la gamme de 246 à 345°C. Les pressions de la réaction utilisées variaient de 167 à 280 cm Hg. La solution d'alimentation était composée de 5,3–9,7 ou 16,5 vol. % de NH_3, la balance étant dans chaque cas O_2. Le flot du réacteur a été analysé par la chromatographie gazeuse et les produits de la réaction étaient N_2, N_2O et H_2O.

On a trouvé que les taux de formation de N_2 et de N_2O dépendaient de p_{NH_3}, p_{O_2} et p_{H_2O} et étaient indépendants de p_{N_2} et de p_{N_2O}. Le taux de croissance de p_{H_2O} a diminué et p_{O_2} a augmenté, pour les deux taux. L'accroissement de p_{NH_3} et de la température ont favorisé la formation de N_2O. Le rendement maximum de N_2O réalisé dans cette opération était d'environ 24%. Le transport de masse en phase gazeuse n'a pas influencé la répartition du produit et n'a pas contrôlé le taux de réaction. Les équations sont développées pour exprimer les taux de formation de N_2 et de N_2O. Ces équations sont envisagées dans un ensemble cinétique comprenant deux réactions paralléles avec O_2 en tant que réactif commun. Des étapes possibles élémentaires, qui constituent les deux réactions d'oxydation, sont analysées suivant les expressions du taux dérivées expérimentalement. Ces dernières sont comparées à celles qui ont été prédites par la théorie du taux absolu et les résultats de l'accord ordre de magnétude.

Zusammenfassung—Die Kinetik der Oxydation von NH_3 mit O_2 über einem Ru-Katalysator von 0,5 Gewichts—%) auf einem Träger von zylindrischem (0,318 cm) Al_2O_3-Granulat wurde in einem Strömungsreaktor mit Rührwerk bei schellem Kreislauf von 98% oder mehr der reagierenden Gasmischung untersucht. Dieser experimentelle Weg reduzierte Temperatur- und Konzentrationsgefälle längs der Katalysatorschicht auf ein Mindestmass und ermöglichte genaue Temperatureinstellung und schnellen Massentransport zur Katalysatoroberfläche. Damit wurden gleichförmig-stetige Reaktionsbedingungen über die ganze Länge des katalytischen Reaktors erreicht.

Die Versuche wurden bei sechs Temperaturen im Bereich von 246–345°C und mit Reaktionsdrücken von 1760–2800 (mm Hg) durchgeführt. Die Gaszufuhr enthielt 5,3, 9,7 oder 16,5 (Volums-%) NH_3 und der jeweilige Rest bestand aus O_2. Das Reaktorabgas wurde mittels Gaschromatographie analysiert, und die Reaktionsprodukte erwiesen sich als N_2, N_2O und H_2O.

Man fand, dass die Entstehungsgeschwindigkeit sowohl von N_2 wie von N_2O von p_{NH_3}, p_{O_2} und p_{H_2O} abhingen und von p_{N_2} und p_{N_2O} unabhängig waren. Erhöhung von p_{NH_3} und Temperatur begüngstigte die Bildung von N_2O. Erhöhung von p_{H_2O} verringerte und p_{O_2} steigerte beide Geschwindigkeiten. Die bei diesen Arbeiten erzielte Maximalausbeute an N_2O betrug 24%. Gasphasen-Massentransport hatte auf die Produktverteilung und Reaktionsgeschwindigkeit keinen Einfluss.

Gleichungen, die die Entstehungsgeschwindigkeiten von N_2 und N_2O ausdrücken, werden entwikkelt. Diese Geschwindigkeitsgleichungen werden als Ausdrücke eines kinetischen Schemas für zwei Parallelreaktionen mit O_2 als gemeinsamen Reagens besprochen. Die möglichen grundlegenden Schritte, die beide Oxydationsreaktionen ausmachen, werden in ihrer Beziehung zu den experimentell abgeleiten Geschwindigkeitsausdrücken analysiert, und diese letzteren mit den von der Theorie der absoluten Geschwindigkeit und durch die Ergebnisse der grössenordnungsmässigen Übereinstimmung vorhergesagten Werten verglichen.